Springer

KSME

Journal of Mechanical Science and Technology 32 (1) (2018) 481~490
www.springerlink.com/content/1738-494x(Print)/1976-3824(Online)
DOI 10.1007/s12206-017-1249-z

CFD analysis of the brake disc and the wheel house through air flow: Predictions of Surface heat transfer coefficients (STHC) during braking operation †

Ali Belhocine[1,*] and Wan Zaidi Wan Omar[2]

[1]*Faculty of Mechanical Engineering, University of Sciences and Technology of Oran, L.P 1505, El - MNAOUER, USTO 31000 ORAN, Algeria*
[2]*Faculty of Mechanical Engineering, Universiti Teknologi Malaysia, 81310 UTM Skudai, Malaysia*

(Manuscript Received March 31, 2017; Revised August 30, 2017; Accepted September 22, 2017)

Abstract

Braking system is one of the basic organs to control a car. For many years, the disc brakes have been used in automobiles for safe retardation of the vehicles. During braking, enormous amount of heat will be generated, and for effective braking, sufficient heat dissipation is essential. The specific air flow surrounding the brake rotor depends on the thermal performance of the disc brake and hence, the aerodynamics is an important in the region of brake components. A CFD analysis is carried out on the braking system as the study of this case, to make out the behavior of air flow distribution around the disc brake components using ANSYS CFX software. The main object of this work is to calculate the heat transfer coefficient (h) of the full and ventilated brake discs as a function of time using the CDF analysis, which will be used later in the transient thermal analysis of the disc in ANSYS Workbench 11.0.

Keywords: CFD; Convection; Disc; Gray cast iron; Heat flux; Heat transfer coefficient

1. Introduction

Today, the founding engineers of cars are currently in an unfailing position of maintaining and improving mechanical safety devices in the face of the increase in the need for highly efficient transport. The essential role of an automotive brake system is to brake or stop the rotating wheel bearing by pressing brake pads against the brake discs [1]. Dufrénoy [2] carried out, a thermomechanical analysis of the disc brake of real geometry taking into account the effect of wear and the variations of surface of contact. Söderberg and Andersson [3] conducted a study while developing a disc-brake pad model to calculate the contact pressure distribution at the pad interface and the rotor. Mahmoudi et al. [4] investigated the effects of using FG materials in the wheel-mounted brake disk R920K for the ER24PC locomotives on its thermo-mechanical behavior are investigated. Choi et al. [5] conducted a study in order to determine the correlation between pad surface deformation, slurry adhesive rate and Coefficient of friction (COF) during friction between felt pad and single -crystal silicon, to analyze the relationship between pad condition and COF. In the work carried out by Öz et al. [6] two excessive worn brake discs of a light commercial vehicle were coated with High velocity oxygen fuel (HVOF) thermal spray process for reuse. Gao and Lin [7] have shown by experience, that the temperature of the contact is an integral factor indicating the influence of powerful friction on the combined effect of charge, velocity, coefficient of friction and thermomechanical properties and the lifetime of the materials. The cone setting or thermal distortion of the disc results from the different distribution in the discs and brake pads according to the works of Lee and Yeo [8]. Park et al. [9] developed a simulation program for automotive cooling system analysis and a performance analysis program for analyzing heat exchanger. Park et al. [10] presented a local Nusselt number in the cooling flow passage of the automobile disc brake with helically fluted surfaces. Chung et al. [11] presented an analysis method to estimate the thermal performance of a disc in a vehicle considering braking conditions. Heat flux is applied to the finite element disc model, and the temperature rise and deformation of a disc are estimated by performing the thermo-mechanical analysis. Duzgun [12] investigated the thermal behaviors of ventilated brake discs using three different configurations of continuous brake conditions in terms of heat generation and thermal stresses with finite element analysis. Belhocine and Bouchetara [13] presented a numerical modeling in three dimensions to analyze the thermal behavior of the brake discs of the vehicles using computing code ANSYS. Luo and Zuo [14] studied the heat dissipation of a ventilated disc on high-speed trains during emergency braking in order to improve heat dissipation performance. Mahmoudi et

*Corresponding author. Tel.: +213 790092648
E-mail address: belho2017@gmail.com
† Recommended by Associate Editor Seong Hyuk Lee
© KSME & Springer 2018

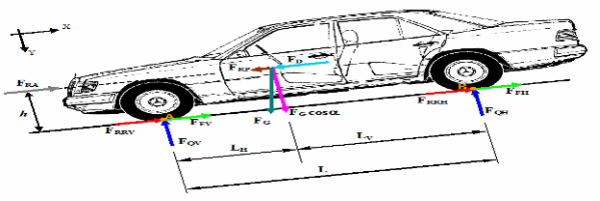

Fig. 1. Definition of the forces acting on an automobile during braking.

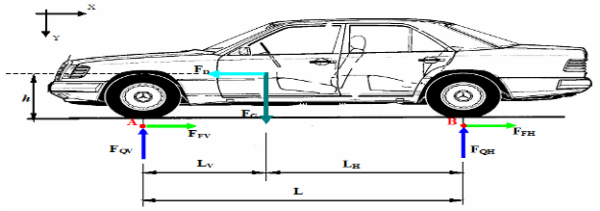

Fig. 2. External forces acting on the vehicle during braking on a flat road.

al. [15] investigated the effects of using FG materials in the wheel-mounted brake disc R920K for the ER24PC locomotive on its thermo-mechanical behavior. Ljungskog et al. [16] investigated the effects of flow angularity at the inlet and different boundary layer control systems, namely, basic scoop suction, distributed suction, and moving belts, on the longitudinal pressure distribution in the full-scale aerodynamic wind tunnel of Volvo Cars using CFD and a systematic design of experiments approach. Recently, Belhocine and Wan Omar [17] have guided a static structural analysis of dry sliding contact between the brake disc and pads using the ANSYS 11.0 finite element software. After that, Belhocine [18] conducted a coupled thermomechanical analysis showing the effect of temperature on the resulting stresses and overall deformations of the disc as well as; contact pressures in the brake pads. The convective heat coefficient (h) mainly depends on the air flow inside and around the brake disc, i.e. ,the flow velocity which generally increases the heat transfer rate. The turbulence intensity usually increases the heat transfer rate through increasing intensity and the flow structure.

The main aim of our work is to calculate the values of the convective heat transfer coefficient (h) using the ANSYS CFX 11.0 software, which must be expressed as a function of time for each surface of the full and ventilated disc and that they will be exploited to the determination of (3D) three-dimensional temperature of the disc under ANSYS Software in transient thermal regime [19]. Thus, the results induced by the analysis, show us the importance of ventilation in the brake disc design.

2. Calculating heat fluxes entering the disc

2.1 The forces acting on the wheels during braking

By observing the situation described in Fig. 1, the longitudinal and transverse equilibrium of the vehicle can be written along the local axes x, y of the car.

$$\sum F_X = 0$$

$$F_{RRV} + F_{FV} + F_{RRH} + F_{FH} + F_{RA} - (F_{RP} + F_D) = 0 \quad (1)$$

$$F_{FV} + F_{FH} = F_{RP} + F_D - F_{RRV} - F_{RA} - F_{RRH} \quad (2)$$

$$F_F = F_{RP} + F_{RF} - F_{RR} - F_{RA} \quad (3)$$

with $F_F = F_{FV} + F_{FH}$, $F_{RR} = F_{RRV} + F_{RRH}$

$$\sum F_Y = 0 \Rightarrow F_G \cos\alpha - (F_{QV} + F_{QH}) = 0 \quad (4)$$

$$F_{QH} = F_G \cos\alpha - F_{QV} \quad (5)$$

$$\sum M_B = 0 \Rightarrow F_{QV} L + F_{RA} h - h(F_{RF} + F_{RP}) - hF_G \sin\alpha \quad (6)$$

$$F_{QV} = \frac{\left[(F_{RF} + F_{RP})h + F_G L_H - F_{RA} h\right]}{L}. \quad (7)$$

On a road vehicle, the rolling force $F_{RR} = F_G$ f$_r$ cos α is due to the flat formed by a tire on the road, f$_r$ is the rolling resistance coefficient. For a high pressure tire (f$_r$ = 0.015)

$$F_{RP} = F_G \sin\alpha \,. \quad (8)$$

The aerodynamic force is given by:

$$F_{RA} = C_X A_F \frac{\rho_a}{2} v^2 \,. \quad (9)$$

With C_X is the coefficient of form, equal to: 0.3 to 0.4 on the car, A_F *(m^2)* is the frontal surface; on the approach, for a road passenger vehicle, we can take:A_F = 0.8×height×width *S,* and ρ_a is the air density.

2.2 Total braking power

$$P_{tot} = P_R + P_F \quad (10)$$

$$\text{By } P_F = \sum F_F v = (F_{FV} + F_{FH})v \quad (11)$$

$$P_R = \sum F_R v = (F_{RR} + F_{RP} + F_{RA})v. \quad (12)$$

In the case of flat braking (Fig. 2), the resistances due to rolling and the slope are neglected ($F_{RR} = 0$ and $F_{RP} = 0$), the penetration into the air is generally negligible, for this reason, ($F_{RA} = 0$)

$$P_R = \sum F_R v = (F_{RR} + F_{RP} + F_{RA})v = 0 \quad (13)$$

$$P_F = \sum F_F v = (F_{FV} + F_{FH})v \quad (14)$$

$$(F_{FV} + F_{FH}) = F_D = ma \quad (15)$$

$$P_{tot} = P_F = m\,a\,v \,. \quad (16)$$

If we define, Let φ the factor of the ratio of the braking power with respect to the rear wheels $P_{FH} = \varphi\, mav$ then, $P_{FV} = (1\text{-}\varphi)mav$

if a is constant, we have:

$$v(t) = v_0 - a\,t \tag{17}$$

$$P_F = (1-\varphi)ma(v_0 - a\,t)\,. \tag{18}$$

The braking power delivered to the brake disc is equal to half the total power:

$$P_{FVI} = \frac{(1-\varphi)}{2}ma(v_0 - a\,t)\,. \tag{19}$$

At time t = 0, we have

$$P_{FVI} = \frac{(1-\varphi)}{2}ma\,v_0\,. \tag{20}$$

The braking efficiency is then defined by the ratio between the deceleration (a) and the acceleration (g):

$$Z = a_d / g \tag{21}$$

$$P_{FVI} = \frac{(1-\varphi)}{2}mZgv_0\,. \tag{22}$$

Assuming that the amount of heat generated by friction is completely absorbed by the disc.

$$Q_v = \frac{(1-\varphi)}{2}m_{tot}\,g\,v \quad [Nm/s] = [W]\,. \tag{23}$$

The expression of the transformed friction power per unit area is thus:

$$Q_v^{'} = \frac{(1-\varphi)}{2}\frac{m_{tot}\,g\,v}{2A_d} \quad [Nm/sm^2] = [W/m^2]\,. \tag{24}$$

The quantity Q'_v indicates the heat flow absorbed by the disc, which must be housed only on the actual contact surface. Where A_d is the surface of the rotor to which a brake pad pivots. By definition, the operating factor ε_p of the friction surface is given by the following formula:

$$\varepsilon_p = Q_v^{'} / Q_{v_{\max}}^{'}\,. \tag{25}$$

Thus, the equation of the initial thermal flow of friction entering the disc, which is calculated as follows:

$$Q_{v_{\max}}^{'} = \frac{(1-\varphi)}{2}\frac{m_{tot}\,g\,v}{2A_d} \quad [Nm/sm^2] = [W/m^2]\,. \tag{26}$$

2.3 Heat flux entering the disc

During braking, each surface of the rotor receives a heat flux from the friction generated at the disc-pads interface. The expression of the initial heat flux entering the disc is given as follows [20]:

Table 1. Basic dimensions and main parameters of automotive braking.

Parameter	Value
Inside diameter of the disc, mm	66
Outside diameter of the disc, mm	262
Disc thickness (TH), mm	29
Disc height (H), mm	51
Weight of the car m, kg	1385
Initial velocity v_0, m/s	28
Deceleration a, m/s^2	8
Time of braking t_b, s	3.5
Effective disc radius R_{disc}, mm	100.5
Ratio braking forces distribution φ, %	20
Factor of disc charge distribution ε_p	0.5
Disc's swept area A_d, mm^2	35993

Table 2. Disc material properties for thermal analysis.

Material properties	Disc
Thermal conductivity, k (W/m°C)	57
Volumetric mass density (kg/m^3)	7250
Specific heat capacity, c (J/Kg. °C)	460
Poisson's ratio	0.28
Thermal expansion (10^{-6} / °C)	10.85
Young modulus, E (GPa)	138

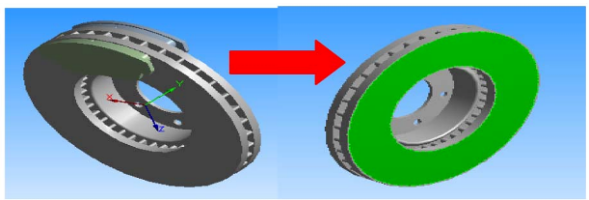

Fig. 3. Application of flux.

$$q_0 = \frac{(1-\varphi)}{2}\frac{m\,g\,v_0\,z}{2A_d\varepsilon_p} \tag{27}$$

where a is the vehicle deceleration [ms^{-2}], $z = a/g$ is the braking effectiveness, and g is the gravity acceleration constant (9.81) [ms^{-2}].

Given the difficulty of the problem treated, we will assume that the brake pads must be replaced by their friction effect and that they must be fictitiously represented by an incoming heat flux (Fig. 3).

In order to allow us to easily compare the results, the concrete dimensions of the two discs (Full and ventilated) are quite similar. The main dimensions of the disc and the parameters involved are summarized in Table 1.

We chose for the brake disc, gray cast iron material (FG 15) of carbon composition [21], better thermomechanical specificities which are summarized in Table 2.

3. CFD analysis with ANSYS CFX

A CFD analysis generates an approximate description of the behavior of physical model, rather than of real physical system. The partial differential equations that usually constitute a physical model are themselves only imprecise models of real behavior. The modeling approximations are typically much larger source of error, we have to use in the equations when dealing with complex phenomena unsuitable for direct numerical analysis. The list is long. It certainly includes turbulence, multiphase flows, and flows with chemical reaction. Properties of real liquids and gases (e.g., Density or viscosity) depends in a complex and not always well documented way on temperature, pressure, concentration of admixtures. This is often neglected in CFD analysis, and the properties are assumed constant. In the case where this assumption is abandoned, the error is still introduced, since the properties are approximated by imprecise empirical functions.

3.1 k-ε turbulent model

One of the most prominent turbulence models, the (k-epsilon) model, has been implemented in most general purpose CFD codes and is considered the industry standard model. It has proven to be stable and numerically robust and has a well-established regime of predictive capability. For general purpose simulations, the model offers a good compromise in terms of accuracy and robustness.

3.2 Modeling assumptions

The following assumptions were made for CFD calculation

- At the inlet, the air velocity was adjusted to 28 m/s.
- The initial speed of the vehicle is 28 m/s.
- The flow medium is air.
- According to a k-ε turbulence model, flow through the rotor is steady incompressible and turbulent.
- Physical properties such as (Density, thermal conductivity, specific heat and viscosity) are constant.
- Only two modes of heat transfer (Conduction and convection) but the radiation effects are neglected.
- On the disc surface, the heat flux is uniform
- Properties of air are taken under standard temperature and pressure conditions,
- Approximately 90 % of frictional heat is transferred to brake disc.

3.3 CFD modeling

Brake rotors are designed to dissipate heat effectively, but air flow inside and around the brake rotor is turbulent in nature. Because of aggressive braking, heat is built up around the brake rotor and the rotor alone is not capable of extracting all the generated heat in a short amount of time. As the practical life shows, brake ducts works by channeling air from the front surface of the car to the brake rotor. Atmospheric air taken in by the brake duct is much cooler than the air around the brake disc. Air flow through the duct continuously moves hot air away, which allows the brake to cool at a faster rate, lowering the operating temperature of the brake assembly.

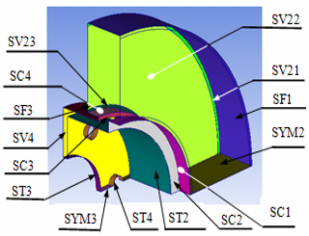

Fig. 4. Full disc faces.

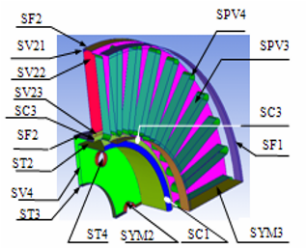

Fig. 5. Ventilated disc faces.

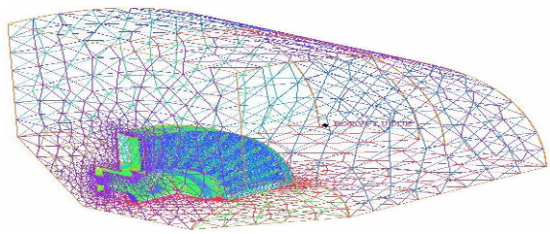

Fig. 6. Meshing for a fluid body.

Using ANSYS ICEM CFD, we have developed the presentation of the internal and external face differences used in the simulation for each full and ventilated disc while distinguishing them with distinct ones to facilitate our calculations as showed in Figs. 4 and 5. Mesh established in the disc is an irregular and non-uniform mesh, so that the meshes are more extended where there are weak gradients. The CFD model of the brake disc was solved by ANSYS-CFX and given the nature of the problem; the boundary conditions for each variable must be imposed on the boundaries of the computational domain. The domain of interaction is considered perfectly adiabatic. The temperature of the air flow and that of the disc is constant and equal to the ambient temperature and they must be set at 30 °C, whose lower and upper and radial ends of the domain have been subjected to zero relative pressure.

3.4 Fluid mesh generation

To allow us to develop the model corresponding to the domain of the fluid which is the air, we adopted a linear

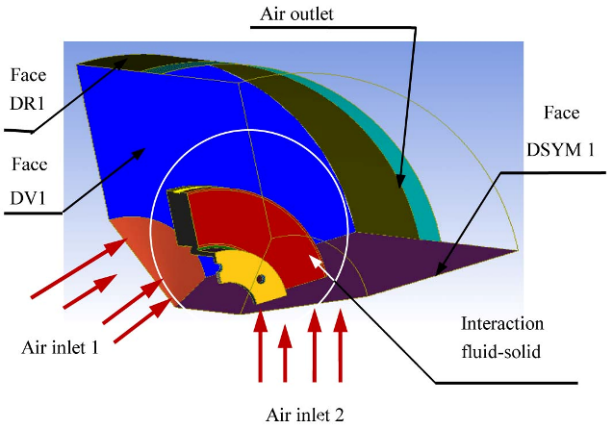

Fig. 7. Fluid body surfaces in ANSYS ICEM CFD.

tetrahedral mesh with 30717 nodes and 179798 elements as illustrated in Fig. 6.

Using the ANSYS ICEM CFD software, and because of the symmetry of the brake disc, only a quarter of the fluid domain was taken into account in the calculations (Fig. 7).

3.5 Boundary conditions and computational details

The flow of air through and round the brake disc was analyzed using the ANSYS CFX code package. Material knowledge was taken from ANSYS material knowledge library for air at 20°C. Our study is carried out on a brake disc in three types of gray cast iron (FG25AL, FG20, FG15) whose thermal conductivities are respectively (43.7 W / m °C, 55 W / m °C and 57 W / m °C). This work presents a thermal study, which was undertaken on the basis of an analysis of a flow of air passing through a disc so that it is possible to follow the scenario of temperature variation and the heating of the rotor during the braking phase. This allows the following time conditions to be entered in ANSYS: Braking time is equal to 3.5 seconds with a time in increments of 0.01 seconds.

Periodic boundary conditions are used when the physical geometry of interest and the expected pattern of the flow/thermal solution have a periodically repeating nature. Periodic boundary conditions are used when the flows across two opposite planes in the computational model are identical. The brake disc rotor is rotationally periodic, i.e. the geometry and the flow pattern repeat themselves at a specified angle to the centerline. Flow exiting one periodic plane is same as the flow entering the other periodic plane. The introduction of periodic boundary (Cyclic symmetry) conditions indicated that only a periodic repetitive a quarter of the disc was modeled rather than the entire disc. This had the effect of making the model much simpler, which translates into a reduction in material requirements and a high amount of calculation time. The implementation of atmospheric temperature and pressure at the inlet and outlet boundaries allows us to model the rotating brake disc in still air. Air rounds the disc is taken into account to be 20 °C and a spread of constant angular speeds

Table 3. Boundary conditions.

Boundary	Boundary condition	Parameters
Inlet	Pressure inlet	Atmospheric pressure and temperature
Outlet	Pressure outlet	Atmospheric pressure and temperature
Domain edges	Symmetry	Symmetry
Disc surface	Wall	293K temperature, thermal properties of Gray cast iron

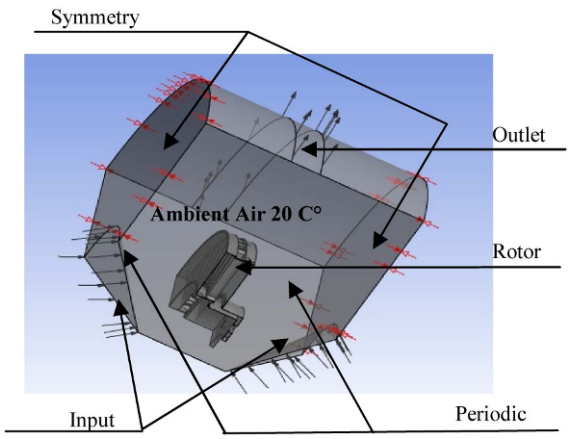

Fig. 8. CFD boundary conditions model.

were sculptured employing a rotating frame of reference regarding the disc and shaft axis. The disc walls are shown as smooth walls at a constant temperature of 293 K. At the domain, we used symmetry boundary conditions to generate zero-shear slip walls. The CFD model derived from the ANSYS CFX code used in the calculation of the film coefficient is illustrated in Fig. 8.

A complete summary of the boundary conditions used is given in Table 3.

4. Results of CFD analysis and discussion

4.1 Steady cases

The results obtained from the calculations for the two discs in the steady state are clearly shown on the Figs. 9-12. In other words, these figures represent the variation of the heat transfer coefficient for brake disc with and without vanes. Since the convective heat transfer coefficient is directly proportional to the heat transfer rate higher the heat transfer coefficient will lead to higher heat transfer rate. The results show that providing vanes obviously increase the heat transfer coefficient.

Figs. 10-12 show the distribution fields of the exchange coefficient (h) for the three types of materials. While comparing the results of material FG25AL, FG20 and FG15, heat transfer coefficient has increased on the surface of the disc in the latter case. That is to say, for the material FG15 the maximum value of the heat transfer coefficient was obtained for it (295 W/m^2 K) and there is no significant variation

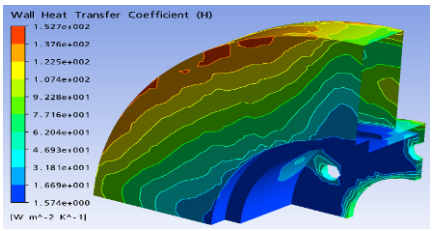

Fig. 9. Wall heat transfer coefficient distribution on a full disc for material (FG 15) at the steady state case.

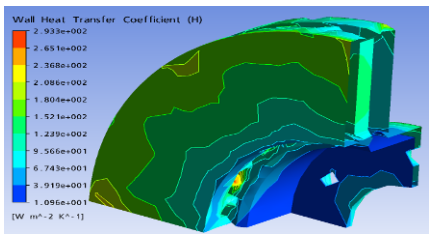

Fig. 10. Wall heat transfer coefficient distribution on a ventilated disc for material (FG 25 AL) at the steady state case.

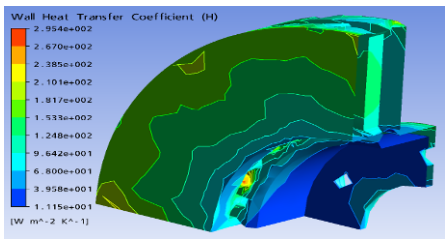

Fig. 11. Wall heat transfer coefficient distribution on a ventilated disc for material (FG 20) at the steady state case.

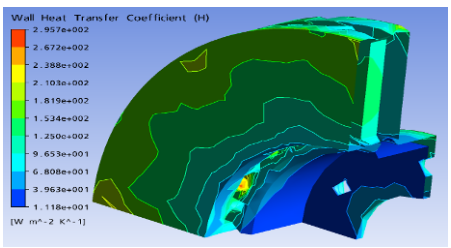

Fig. 12. Wall heat transfer coefficient distribution on a ventilated disc for material (FG 15) at the steady state case.

obtained from the heat transfer coefficient for the three materials. It is found that the behavior of (h) in the disc does not depend on the material chosen. The distribution of (h) in the disc is the same as that existing in the literature. By providing vanes in the disc and in a FG15 design material, the cooling rate increases significantly this ultimately causes energy dissipation which is higher in the case of other types of materials (FG25 AL and FG 20). It is then concluded that the ventilated disc made with the gray cast iron FG15 represents a better cooling.

Table 5 shows the mean values of the convective heat transfer coefficient (h) calculated by the minimum and maximum values of the various surfaces of the ventilated disc.

Table 4. Value of the heat transfer coefficient of different surfaces in the stationary case for a full disc (FG 15).

	FG 15
Surface	$h_{average}$ = [W m^{-2} k^{-1}]
SC1	25
SC2	5
SC3	2
SC4	11
SF1	111
SF3	53
ST2	23
ST3	65
ST4	44
SV1	81
SV2	71
SV3	41
SV4	65

Table 5. Value of the heat transfer coefficient of different surfaces in the stationary case for a ventilated disc (FG 25 AL, FG 20 and FG15).

Materials	FG 25 AL	FG 20	FG15
Surface	$h_{average}$ = [W m^{-2} k^{-1}]		
SC1	54	53	53
SC2	84	83	83
SC3	44	44	44
SF1 and 2	135	135	135
SF3	97	95	94
SPV1	170	171	171
SPV2	134	134	134
SPV3	191	191	192
SPV4	175	176	176
ST1	113	114	114
ST2	35	34	34
ST3	68	66	66
ST4	75	72	71
SV1	135	131	131
SV2	119	118	118
SV3	46	44	44
SV4	111	108	108

It is found that the type of the material does not have a great influence on the variation of the convective heat transfer coefficient (h). Contrary to the first case, it is found that the value of the heat exchange coefficient (h) is strongly influenced by the ventilation system for the same material (FG 15).

4.2 Transient cases

Figs. 13 and 14 illustrate the evolution of the convective

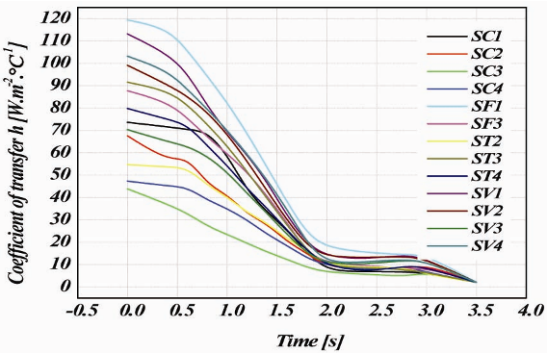

Fig. 13. CFD simulation results of convective heat exchange coefficient *(h)* for different full disc faces in transient mode of material (FG 15).

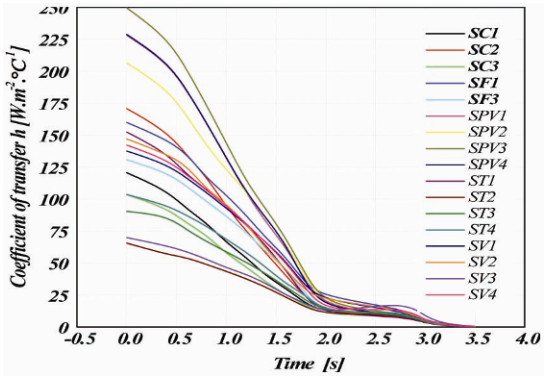

Fig. 14. CFD simulation results of convective heat exchange coefficient *(h)* for different ventilated disc faces in transient mode of material (FG 15).

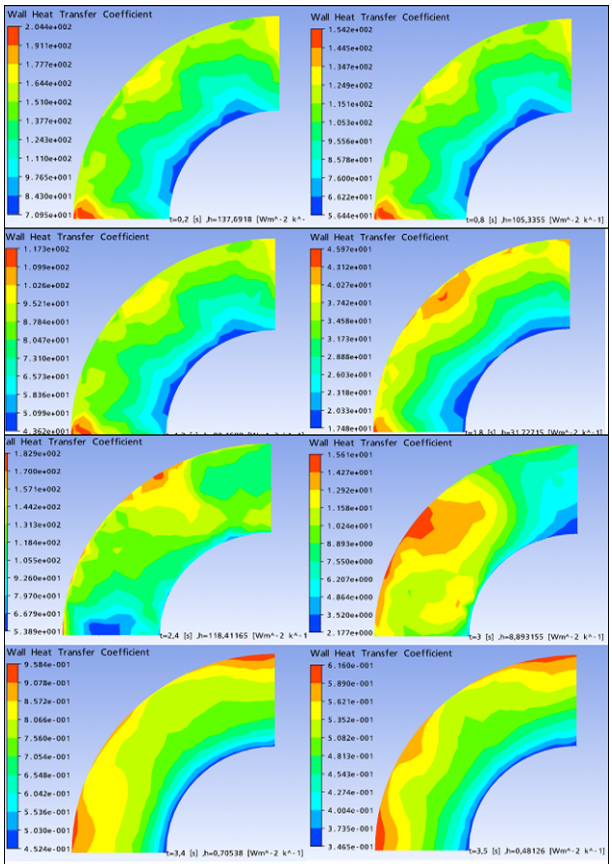

Fig. 15. Variation of the heat transfer coefficient (*h*) on the surface (SV1) and as a function of time for a full disc (FG 15).

coefficient of exchange as a function of time for each face of the full and ventilated disc. These curves should be used in the following to evaluate the three-dimensional temperature of the two discs. It is observed that the geometric design of the full disc is varied towards a ventilated disc, the values of this coefficient also vary with this modification, it is quite reasonable because the ventilation leads to the reduction of the maximum temperatures of the walls.

In Figs. 15 and 16, the variation of the convective thermal coefficient of the wall as a function of time for the faces SV1 and SPV2 belonging, respectively to the full and disc ventilated disc and for the same material FG15. Looking new at external surface heat dissipation, Fig. 15 shows that there is a color degradation (Blue, green and then red) from inlet to outlet of air flow. There is a strong increase in (*h*) towards the circumferential position and the air circulates around the hot section and the variation in the (*h*) values is significant in the upper section of the outboard friction surface of the full disc with very high values at the instant of start of braking t = 0.2 s and then 154 W/m^{2}K at the instant t = 0.8 s, reaching the value 173 W/m^{2}K at the instant t = 1.2 s. While the bottom section of the outboard friction surface of the full disc remains at zero values at time 3.4 s and 3.5 s. Indeed, the values of higher heat transfer coefficients are a characteristic of the beginning of a boundary layer, but these extreme values are present in both the beginning and end regions of the flux and are of an order of magnitude greater than the average on the friction surface. It will be said that the phenomenon of heat dissipation is low in the case of a full disc where the absence of air movement prevents the convection process from occurring, hence the low predicted coefficient value.

Ventilated discs consisting of two rubbing surfaces separated by straight radial vanes are normally employed as they utilize a greater surface area to dissipate heat. By removing the faces of the rotor, Fig. 16 shows the variability of the convective dissipation within and from the channels. The largest values of (*h*) are observed on the lower walls of the channel, reaching 315 W/m^{2}K at time t = 0.2 s. In the air recirculation regions, where heat transfer is reduced, a low heat transfer is also observed in Vanes between 0 ° and 45 °, reaching only 0.6 W/m^{2}K at time t = 3.5 s.

It indicates that the ventilation channels have a positive effect on reducing the temperature. The most possible explanation is when the ventilated disc with large number of vanes is used in brake system; the circulation of air flow tends to cool the hot disc more quickly. Based on physical point of view, the decrease in temperature range, which occurs during braking leads to the increase in the efficiency of braking. This will

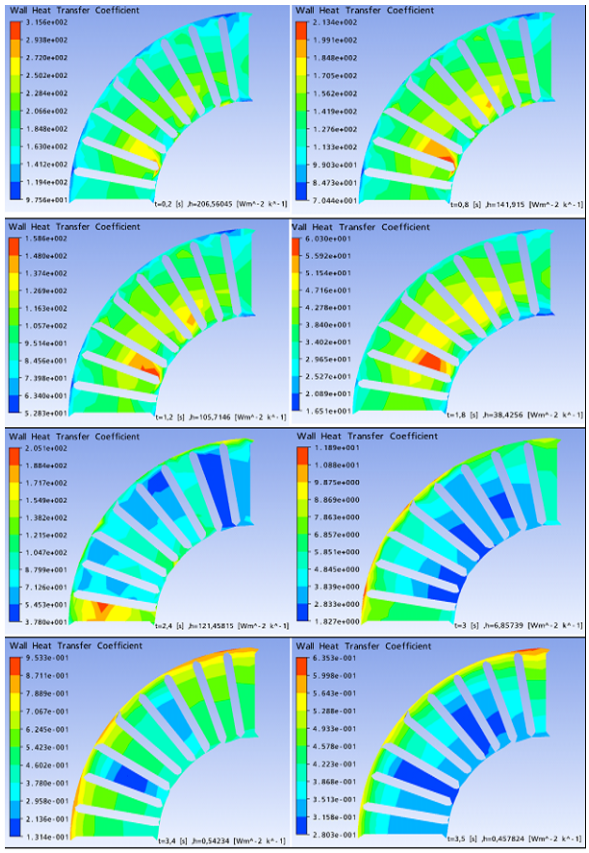

Fig. 16. Variation of the heat transfer coefficient (h) on the surface (SPV2) and as a function of time for a ventilated disc (FG 15).

prevent the possibility of the change of brake fluid phase to the other phase (Vapor). As is known that when the liquid phase changes to the vapor phase, the so called as brake failure will occur and as a consequence this will endanger the driver and the passenger.

It is finding out that for ventilated model the minimum temperature is attained in 42 °C while as for full disc it is 64 °C. This proves that ventilated disc design is more efficient than the full disc in heat dissipation.

5. Mesh of disc brake model

The step of generating the mesh of the structure in the Workbench simulation is essential. For more accurate results in critical areas, we need to refine the mesh in the friction tracks of the brake disc where the brake pads pivot. Using the ANSYS software, we carried out a finite element mesh from the two discs shown in Fig. 17; a full mesh disc in 172103 nodes and 114421 elements and a ventilated mesh disc of 154679 nodes and 94117 elements.

6. Simulation FEM results and discussions

6.1 Results of the disc temperature

On the Figs. 18 and 19, we have shown for each type of

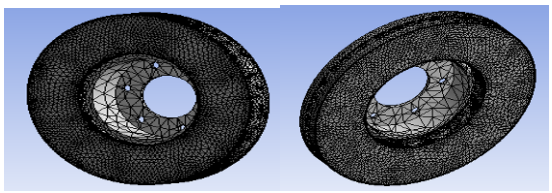

(a) (b)

Fig. 17. Refined mesh on disc friction tracks: (a) Full disc; (b) ventilated disc.

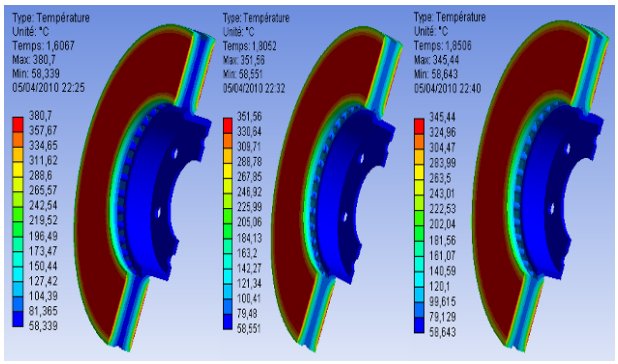

(a) (b) (c)

Fig. 18. Results of thermal analysis of ventilated model for the three materials types: (a) FG 25 AL; (b) FG 20; (c) FG 15.

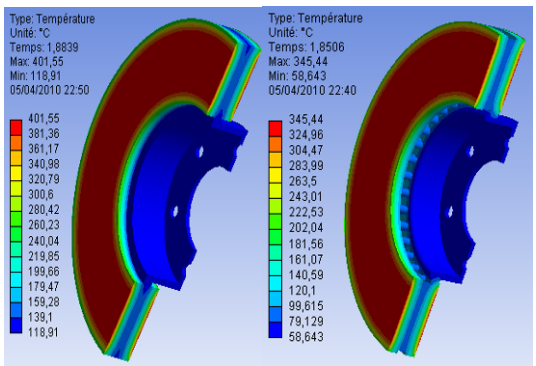

(a) (b)

Fig. 19. Contour of the two discs temperature distribution for material (FG15): (a) Full disc; (b) ventilated disc.

material selected (FG 25 Al, FG 20, FG 15), the evolution of the temperature of the disc at the moment when it is reached. In order to investigate the temperature histories, surface of the disc is selected, because the surface area is subjected to high temperature. These values are gradually reduced from the outer edge to the inner edge. The disc material which has low thermal conductivity results in a temperature rise on the disc surface. It can be seen, that the material FG 15 has a maximum temperature (345 °C) lower than those of the other materials FG 25 AL and FG 20, respectively, of temperatures 380 °C and 351 °C. From this figure, and by comparing the different results obtained from FEA method, it is observed that the rotor disc of gray cast iron FG15 is the best suitable

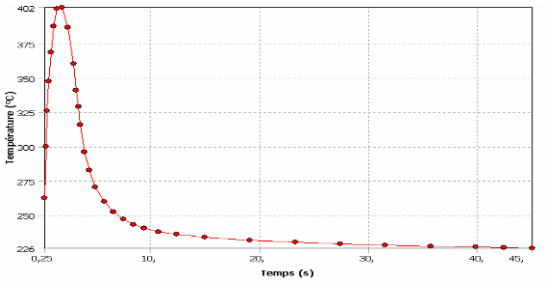

Fig. 20. Evolution of full disc temperature with braking time for material (FG 15).

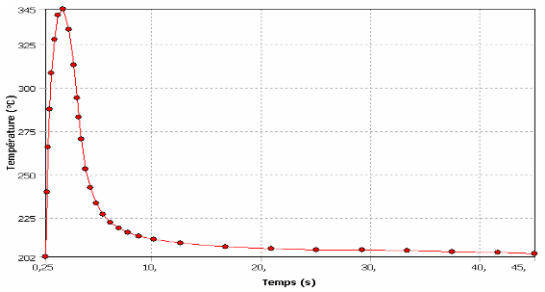

Fig. 21. Evolution of ventilated disc temperature with braking time for material (FG 15).

rotor disc. It is then established the material of gray cast iron FG15 having a better thermal behavior. The full disc temperature reached its apogee value 401 °C at time t = 1.8 s, and then decreases exponentially to 4.9 s on reaching the end of braking (t = 45 s). The maximum temperature rise is indicated in red color and green color shows average temperature rise at the friction surface around the circumference of the disc as shown in Fig. 19, which visually indicates that the ventilated disc is less heated than the full disc. After releasing the brakes, after 1.8506 seconds, the maximum value of temperature in the ventilated disc is 345 °C, which is substantially less than in the case of the full disc. The reason for that is the space between the vanes, which increases heat dissipation from the disc. It may be noted that the ventilated disc is a better solution because the heat is much better drained from its surface. Vanes geometry and their total number greatly affect the heat dissipation from the brake disc. The maximum disc surface temperature results for full and ventilated disc are shown in Figs. 20 and 21 which it illustrates that the time difference [0-3.5 s] indicates the forced convection cycle. Free convection is carried out at the end of the latter until the simulation time limit (t = 45s). It can be seen that the simulation results were similar at the beginning. The reason is that the heat conduction and convection cannot dissipate the huge amount of heat inputted in a short time. It is observed that the ventilated disc having a reduced temperature of almost 60 °C compared to a full disc. It illustrates that the maximum temperature of the full disc was higher than that of the ventilated one. Furthermore, the temperature distribution for the friction ring section (Inboard and outboard) of discs, the ventilated disc was similar to that of the full disc. We conclude that ventilated brake discs in the vehicle design represent a good ventilation system and best means of cooling and then decrease temperatures better than full discs. In summary, it reveals that whilst the ventilated disc can provide better cooling performance is also and maintains similar temperature distribution characteristics to that of a full disc.

7. Conclusion

The present work presents a complex brake disc model to determine the values of the heat exchange coefficient by convection (h) during the phase and braking conditions of the vehicle using the ANSYS CFX software. On the other hand, the numerical results of this investigation were exploited to solve the transient thermal scenario reacted in full and ventilated brake discs where their three-dimensional temperature was visualized using ANSYS Multiphysics 11.0 finite element software. The purpose of the contribution is to show the impact of ventilation in the cooling of discs in service which gives better thermal resistance by guaranteeing a better service life of these. Generally the present study can provide a useful design tool and improve brake performance of a disc brake system. Based on the results of the analysis, it is concluded that:

- All the values obtained from the analysis are less than their allowable values. Brake disc design is safe based on the strength and rigidity criteria.
- Thermal loads, heat flux and single stop temperature rise are calculated with the help of vehicle specifications.
- Maximum temperature rise obtained from FEA analysis for the three¬ different materials, i.e. gray cast iron FG25AL, FG20 and FG15 are 380 °C, 351 °C and 345 °C, respectively.
- Comparing the results of temperature rise obtained from analysis, it is observed that the values are less in the case of material FG 15 than the other materials. It can be concluded that gray cast iron FG15 is the most appropriate material for brake disc.
- The ventilated brake disc is a better solution,because it contains additional surfaces from which the heat dissipates. Disc brake design plays an important role in heat transfer.

As a conclusion, one could say that the numerical results of this simulation are quite adequate compared to what can be found in the literature. It is recommended that the same problem be solved on the experiment as an example through the test benches in order to validate the numerical model to match the current reality.

References

[1] T. Valvano and K. Lee, An analytical method to predict thermal distortion of a brake rotor, *SAE 2000-01-0445* (2000).

[2] P. Dufrénoy, Two-/three-dimensional hybrid model of the thermomechanical behaviour of disc brakes, *J. Rail Rapid Transit Part F,* 218 (2004) 17-30.
[3] A. Söderberg and S. Andersson, Simulation of wear and contact pressure distribution at the pad to-rotor interface, in the disc brake using general purpose finite element analysis software, *Wear,* 267, 12 (1) (2009) 2243-2251.
[4] T. Mahmoudi, A. Parvizi, E. Poursaeidi and A. Rahin, Thermo-mechanical analysis of functionally graded wheel-mounted brake disk, *J. of Mech. Sci. and Technol.,* 29 (10) (2015) 4197-4204.
[5] A. Öz, H. Gürbüz, A. K. Yakut and S. Sağiroğlu, Braking performance and noise in excessive worn brake discs coated with HVOF thermal spray process, *J. of Mech. Sci. and Technol.,* 31 (2) (2017) 535-543.
[6] W. Choi, S. Kim, S. Choi and E. Lee, Pad surface and coefficient of friction correlation analysis during friction between felt pad and single-crystal silicon, *J. of Mech. Sci. and Technol.,* 30 (7) (2016) 3113-3118.
[7] C. H. Gao and X. Z. Lin, Transient temperature field analysis of a brake in a non-axisymmetric three-dimensional model, *J. Materials Processing Technology*, 129 (2002) 513-517.
[8] S. Lee and T. Yeo, Temperature and coning analysis of brake rotor using an axisymmetric finite element technique, *Proc. 4th Korea-Russia Int. Symp. on Science & Technology*, 3 (2000) 17-22.
[9] K. S. Park, J. P. Won and H. S. Heo, Thermal flow analysis of vehicle engine cooling system, *J. of Mech. Sci. and Technol.,* 16 (7) (2002) 975-985.
[10] S. B. Park, K. S. Lee and D. H. Lee, An investigation of local heat transfer characteristics in a ventilated disc brake with helically fluted surfaces, *J. of Mech. Sci. and Technol.,* 21 (2007) 2178-2187.
[11] W. S. Chung, S. P. Jung and T. W. Park, Numerical analysis method to estimate thermal deformation of a ventilated disc for automotives, *J. of Mech. Sci. and Technol.,* 24 (11) (2010) 2189-2195.
[12] M. Duzgun, Investigation of thermo-structural behaviors of different ventilation applications on brake discs, *J. of Mech. Sci. and Technol.,* 26 (1) (2012) 235-240.
[13] A. Belhocine and M. Bouchetara, Thermal behavior of full and ventilated disc brakes of vehicles, *J. of Mech. Sci. and Technol.,* 26 (11) (2012) 3643-3652.
[14] Z. Luo and J. Zuo, Conjugate heat transfer study on a ventilated disc of high-speed trains during braking, *J. of Mech. Sci. and Technol.,* 28 (5) (2014) 1887-1897.
[15] T. Mahmoudi, A. Parvizi, E. Poursaeidi and A. Rahi, Thermo-mechanical analysis of functionally graded wheel-mounted brake disk, *J. of Mech. Sci. and Technol.,* 29 (10) (2015) 4197-4204.
[16] E. Ljungskog, S. Sebben, A. Broniewicz and C. Landström, A parametric study on the influence of boundary conditions on the longitudinal pressure gradient in CFD simulations of an automotive wind tunnel, *J. of Mech. Sci. and Technol.,* 31 (6) (2017) 2821-2827.
[17] A. Belhocine and W. Z. Wan Omar, Three-dimensional finite element modeling and analysis of the mechanical behavior of dry contact slipping between the disc and the brake pads, *Int. J. Adv. Manuf. Technol.,* 88 (1-4) (2017) 1035-1051.
[18] A. Belhocine, FE prediction of thermal performance and stresses in an automotive disc brake system, *Int. J. Adv. Manuf. Technol.,* 89 (9-12) (2017) 3563-3578.
[19] L. Zhang, Q. Yang, D. Weichert and N. Tan, Simulation and analysis of thermal fatigue based on imperfection model of brake discs, Beijing Jiaotong University, *PAMM Proc. Appl. Math. Mech.,* 9 (2009) 533-534.
[20] J. Reimpel, *Braking Technology,* Vogel Verlag, Würzburg (1998).
[21] P. F. Gotowicki, V. Nigrelli and G. V. Mariotti, Numerical and experimental analysis of a pegs- wing ventilated disk brake rotor, with pads and cylinders, *10 th EAEC Eur. Automot. Cong - Paper EAEC05YUAS04-* P 5, June (2005).

Ali Belhocine received his Ph.D. degrees in Mechanical Engineering at the University of Science and the Technology of Oran (USTO Oran), Algeria. His research interests include Automotive Braking Systems, Finite Element Method (FEM), ANSYS simulation, CFD Analysis, Heat Transfer, Thermal-Structural Analysis, Tribology and Contact Mechanic.

Wan Zaidi Wan Omar is now a Senior Lecturer in the Department of Aeronautical, Automotive and Off-shore Engineering, Universiti Teknologi Malaysia. He graduated B.Sc. Engineeing (Aeronautical Eng.) from University of Manchester and M.Sc. Applied Instrumentation and Control from Glasgow Caledonian University. His general research interests are Aircraft Sructures, Aircraft Designand Renewable Energy. His current projects are Design of future ground attack or close air support aircraft, Wind energy systems and Solar powered chiller systems. One of his off-academic end eavour is his fascination with the life and methods of bees - he is now trying to capture a wild honey bee colony from somewhere on Universiti Teknologi Malaysia campus.